CIRP Annals - Manufacturing Technology 71 (2022) 89–92

Contents lists available at ScienceDirect

CIRP Annals - Manufacturing Technology

journal homepage: https://www.editorialmanager.com/CIRP/default.aspx

# Exploratory investigation of chip formation and surface integrity in ultra-high-speed gear hobbing

Yuki Ueda[a], Noriyuki Sakurai[b], Tatsuro Takagi[b], Kazuyuki Ishizu[b], Jiwang Yan (2)[a,*]

[a] Department of Mechanical Engineering, Keio University, Yokohama 223-8522, Japan
[b] Nidec Machine Tool Corporation, Ritto, Shiga 520-3080, Japan

ARTICLE INFO

*Article history:*
Available online 12 April 2022

*Keywords:*
Gear hobbing
Chip formation
Surface integrity

ABSTRACT

Gear hobbing is widely employed to manufacture automotive gears, where the productivity depends on the cutting speed. Currently, gear hobbing is performed at ~300 m/min using high-speed steel hob cutters. In this study, ultra-high-speed gear hobbing was attempted using a large-diameter cemented carbide hob cutter on a gear grinder. This enabled a cutting speed up to 2450 m/min. Many interesting phenomena were acquired in this speed range. Chips were severely oxidized, whereas the gear surface was not affected. Compressive residual stress was generated at the gear surfaces with low surface roughness and high hardness, while the wear of hob cutter was insignificant.



## 1. Introduction

Gear hobbing is widely used to manufacture gears for various products such as automobiles and reduction drives of robots; therefore, gear hobbing has been researched for decades [1,2]. Currently, gear hobbing is performed using high-speed steel (HSS) cutters on conventional hobbing machines. The cutting speed had been limited to < 100 m/min in the past [3] and was increased to ~300 m/min recently. After hobbing, grinding or shaving are performed to improve the gear surface quality [4,5]. The multiple processes reduce the total productivity, making it difficult to ensure good quality. In recent years, carbide, cermet, and PCBN cutters have been utilized in gear hobbing for a high cutting speed > 2000 m/min [6–8]. However, previous studies on ultra-high-speed hobbing have focused on the tool wear characteristics, while the hobbing mechanism at the high cutting speed has not been clarified.

In this study, gear hobbing experiments were conducted at a cutting speed up to 2450 m/min, and the mechanisms of chip/surface formation were investigated. To realize an ultra-high cutting speed, a large-diameter cemented carbide hob cutter was used on a gear grinder. The cutting phenomena including chip morphology, element composition, chip/tool/workpiece temperature, residual stress, surface hardness, and strain distribution of gear surfaces were examined by comparing their results for different cutting speeds. The advantages and challenges of ultra-high-speed hobbing were identified.

## 2. Experimental methods

The workpiece material used in this study was SCM415, a Cr–Mo steel having a tensile strength of 610 N/mm$^2$ and hardness of 180 HBW. The specifications of the gear used for the hobbing experiment are module 1.7 mm, the number of teeth 39, face width 13.4 mm, and tooth depth 5.3 mm. The material of the hob cutter was cemented carbide WC-Co. As shown in Table 1, two types of WC-Co cutters with diameters 65 and 130 mm and gash numbers of 20 and 30 were used. The 65 mm cutter was used on GE15A (No. 1) and GE15HS (No. 2) hobbing machines for the cutting speeds ($V_c$) of ~400 and ~1200 mm/min, respectively. The 130 mm cutter was used on a high-speed gear grinder ZE15B (No. 3) that has a maximum spindle rotation of 6000 rpm, enabling ultra-high-speed cutting at ~2450 m/min. All the machines were produced by Nidec Machine Tool Corp., Japan. The axial feed ($f$) was varied from 0.3 to 7.0 mm/rev. During hobbing, a thermography camera (emissivity 0.97, framerate 15 fps, wavelength 8–14 $\mu$m, resolution 0.025 °C) was used to measure the temperatures of the cutting chips, workpiece, and cutter. The experiment parameters are shown in Table 1. Photographs of the main sections of machine Nos. 2 and 3 are provided in Fig. 1.

**Table 1**
Experimental parameters.

| Machine | | No.1 GE15A | No.2 GE15HS | No.3 ZE15B |
|---|---|---|---|---|
| Hob cutter | Diameter [mm] | 65 | 65 | 130 |
| | Number of threads | | 1 | |
| | Number of gashes | 20 | 20 | 30 |
| Workpiece | Module | | 1.7 | |
| | Helix angle [deg] | | -35 | |
| | Number of teeth | | 39 | |
| | Face width [mm] | | 13.4 | |
| | Tooth depth [mm] | | 5.3 | |
| Cutting condition | Cutting speed $V_c$ [m/min] | 200–400 | 400–1200 | 1001–2450 |
| | Axial feed $f$ [mm/rev] | 0.3–5.0 | 0.3–7.0 | 0.3 |

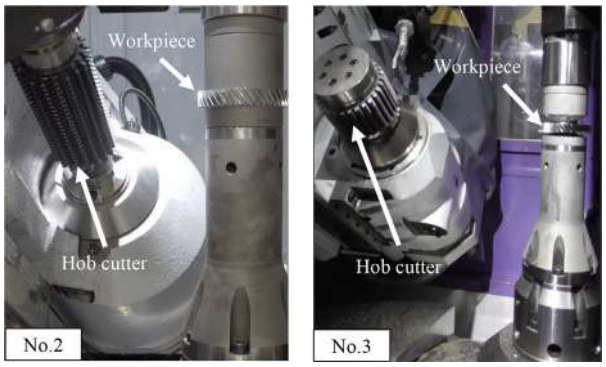


**Fig. 1.** Photographs of gear hobbing machine Nos. 2 and 3.

* Corresponding author.
*E-mail address:* yan@mech.keio.ac.jp (J. Yan).

https://doi.org/10.1016/j.cirp.2022.03.030
0007-8506/

After hobbing, the chips and gear surfaces were analyzed using a scanning electron microscope (SEM) and energy dispersive X-ray spectrometer (EDX) at an acceleration voltage of 5–10 kV. Cross-sectional samples of chips were made using focused ion beam equipment and were observed using a transmission electron microscope (TEM) at an acceleration voltage of 200 kV. The residual stress on the gear surface was measured using a portable X-ray diffraction (XRD) equipment (tube material Cr), where the conditions were set to be spot size 0.8 mm, incidence angle 28.8 °, distance 50 mm, and time 80 s. Gear surface hardness was measured using a micro-Vickers hardness tester. Cross-sectional samples of the gear surfaces were prepared by polishing, and the strain distribution of the samples were characterized by electron backscattering patterns (EBSD) at an acceleration voltage of 15 kV.

## 3. Results and discussion

### 3.1. Chip morphology observation

Fig. 2 shows photographs of the cutting chips obtained at different cutting speeds and axial feeds from different machines. As the cuspeed increases, the chip color changes from silver (Fig. 2(a)) to brown (Fig. 2(b)) and then to dark blue (Fig. 2(c)). Similarly, the increase in axial feed causes the thicker parts of the chips to change to dark blue, and with further increase, the entire chip becomes blue (Fig. 2(d–f)).

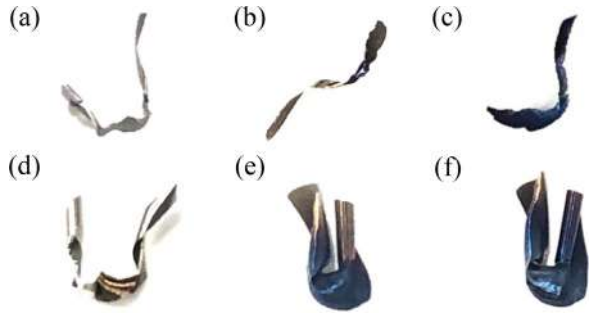


**Fig. 2.** Color change of cutting chips: (a) No. 1, $V_c$ = 200 m/min, $f$ = 0.3 mm/rev; (b) No. 2, $V_c$ = 1000 m/min, $f$ = 0.3 mm/rev; (c) No. 3, $V_c$ = 2450 m/min, $f$ = 0.3 mm/rev; (d) No. 1, $V_c$ = 400 m/min, $f$ = 1.0 mm/rev; (e) No. 1, $V_c$ = 400 m/min, $f$ = 3.0 mm/rev; (f) No. 1, $V_c$ = 400 m/min, $f$ = 5.0 mm/rev.

Fig. 3 shows the SEM images of the surfaces of the cutting chips obtained at the same axial feed of 0.3 mm/rev for different cutting speeds. At 400 and 1200 m/min, the chip surfaces are composed of lamellar structures (Fig. 3(a) and (b)). At 2001 m/min, however, the chip surface is roughened and covered with a network of while lines (Fig. 3(c)). At 2450 m/min, the roughness of the chip surface increases and exhibits a granular structure (Fig. 3(d)).

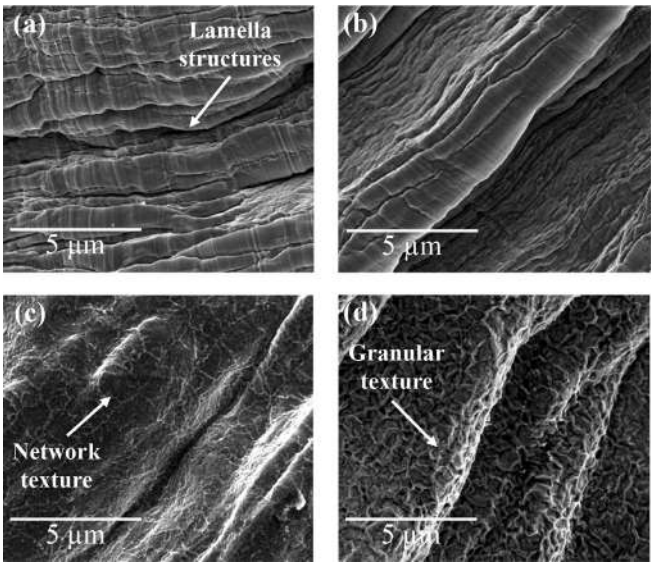


**Fig. 3.** SEM images of chip surfaces: (a) No. 2, $V_c$ = 400 m/min; (b) No. 2, $V_c$ = 1200 m/min; (c) No. 3, $V_c$ = 2001 m/min; (d) No. 3, $V_c$ = 2450 m/min. $f$ = 0.3 mm/rev for (a)–(d).

### 3.2. Composition analysis

Fig. 4 illustrates the cross-sectional EDX mapping results of the chip shown in Fig. 3(d). A thick film covers the chip body, inside which there are numerous tiny holes. In addition, there is a small gap between the chip body and film. The mapping results show that the thick film is rich in O and Fe, while a very thin layer of the chip body is rich in Cr. This indicates that the Fe element in the chip diffused outside the chip body and was preferentially oxidized, separating Fe from other stable elements such as Cr and Si. These stable elements were deposited at the boundary between the chip body and iron oxide film. The iron oxide film caused the dark blue color and a roughened granular surface.

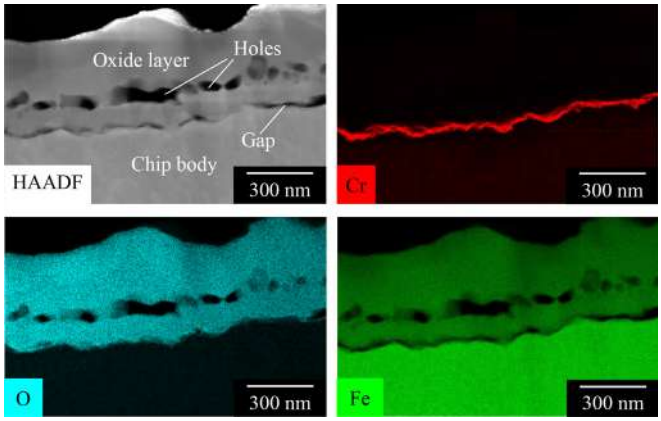


**Fig. 4.** Cross-sectional EDX mapping of a chip obtained at $V_c$ = 2450 m/min and $f$ = 0.3 mm/rev using machine No. 3.

Fig. 5(a) and (b) present the element analysis results for the surfaces of chips and workpieces, respectively, obtained for various cutting speeds. As the cutting speed increases, the percentage content of oxygen increases for the chip (Fig. 5(a)), while there is almost no change in the oxygen content for the workpiece surface (Fig. 5(b)). This indicates that although the chips were severely oxidized, the workpiece was almost unaffected.

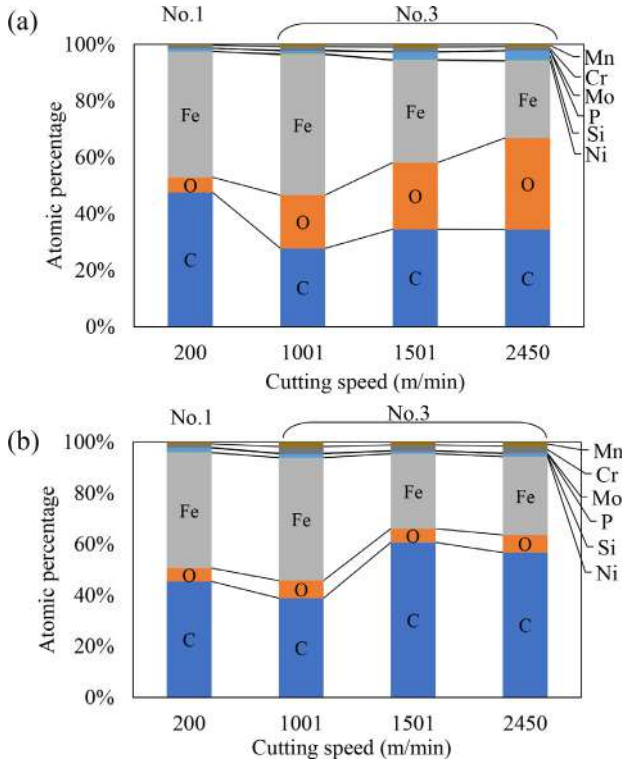


**Fig. 5.** Element analysis for the surfaces of (a) chip and (b) workpiece machined at $f$ = 0.3 mm/rev using machine Nos. 1 and 3.

### 3.3. Temperature measurement

The temperatures of the cutting chips, workpiece, and hob cutter measured during the hobbing experiment using machine No. 2 are shown in Fig. 6. As cutting speed increases, the temperature of the cutting chips increases significantly, while there is only a slight temperature rise in the workpiece and hob cutter. These results indicate that the cutting heat has been mainly brought away by chip removal, which causes chip surface oxidation, whereas the heat conduction into the tool and workpiece was insufficient to cause a notable rise in temperature. The temperature of the chips was measured after being ejected from the gear grooves and deposited in a box; the temperatures of the cutter and workpiece were measured during their rotation; hence, the measured temperatures are lower than the local temperature of the cutting point.

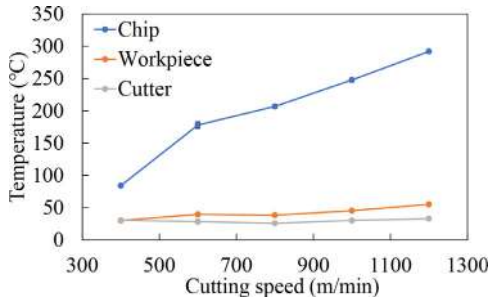


**Fig. 6.** Temperature change of chip, cutter, and workpiece with cutting speed (No. 2, $f$ = 0.3 mm/rev).

### 3.4. Surface roughness

Fig. 7 shows a plot of surface roughness versus cutting speed. Generally, the cutting speed has negligible effect on the change in surface roughness. The surface roughness of the gears hobbed by the cemented carbide cutters is of the order of 0.1 $\mu$m Ra, which is considerably lower than that obtained by a HSS cutter (~1 $\mu$m Ra) and comparable to that finished by gear shaving with a PVD-coated HSS tool (~0.16 $\mu$m Ra) [1]. This demonstrates the feasibility of ultra-high-speed hobbing using a cemented carbide cutter to produce smooth gear surfaces without adopting subsequent finishing processes.

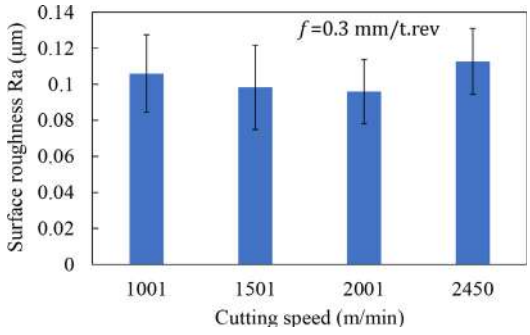


**Fig. 7.** Change in surface roughness with cutting speed (machine No. 3).

### 3.5. Residual stress

The XRD analysis result of the residual principal stress in the gear surface along the gear tooth profile direction is shown in Fig. 8. In the range of $V_c$< 800 m/min, the tensile stress increases as the cutting speed increases. When $V_c$> 1000 m/min, however, the compressive residual stress is dominant and increases with the cutting speed. A compressive residual stress of 123 MPa was achieved at $V_c$ = 2001 m/min. The curve discontinuity at 800–1000 m/min is due to the difference in hob cutter diameter, which induces different uncut chip thickness.

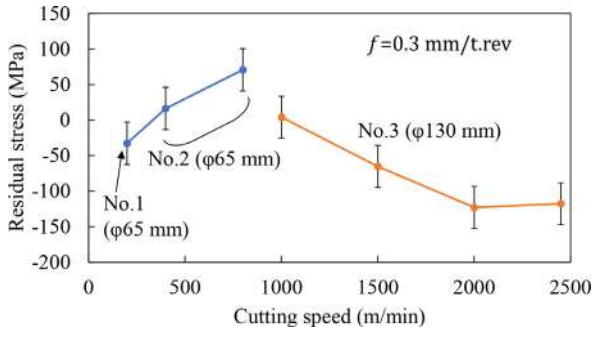


**Fig. 8.** Variation of residual stress in gear surface with cutting speed.

### 3.6. Surface hardness

To explore the mechanical property of the hobbed gear surface, hardness tests were conducted using a micro-Vickers indenter at a load of 980 mN. To eliminate the random error, five indentations were made for each sample, and the results were averaged. As shown in Fig. 9, the gear surface hardness decreases suddenly as cutting speed increases in the range of $V_c$< 800 m/min. When $V_c$> 1500 m/min, the surface hardness increases gradually with cutting speed. The trend exhibited by the surface hardness in Fig. 9 is reverse to that of the residual stress in Fig. 8. This indicates a close correlation between residual stress and hardness; the stronger the compressive stress, the higher the surface hardness. Similar trends were reported for the cutting of carbon steels [9]. The discontinuous change at 800–1000 m/min was caused by the difference in the diameters of the hob cutters.

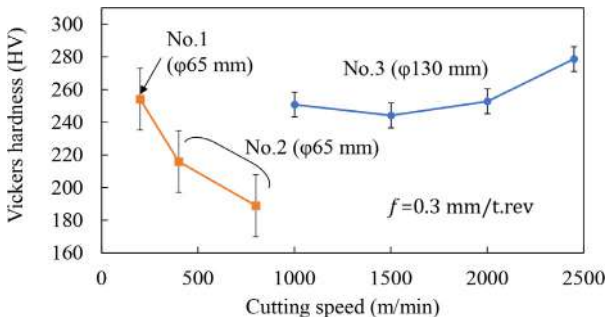


**Fig. 9.** Variation of gear surface hardness with cutting speed.

### 3.7. Surface strain characterization

To explain the changes in the residual stress and hardness of the gear surface, a cross-sectional sample of the gear tooth was characterized using EBSD. Fig. 10 shows the backscattered electron (BSE) images and Kernel average misorientation (KAM) mappings of the gear surfaces obtained at different cutting speeds. At $V_c$ = 200 m/min, the strain is distributed in a wide range to a depth of approximately 10 $\mu$m from the surface. In contrast, at $V_c$ = 2450 m/min, the strain is concentrated within a thinner layer (thickness ~5 $\mu$m). The results in

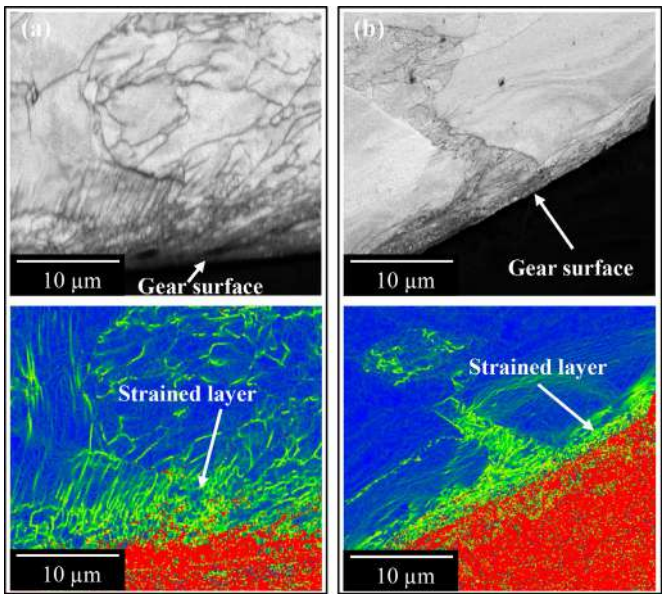


**Fig. 10.** BSE images and KAM mappings of gear surfaces: (a) No. 1, $V_c$ = 200 m/min, $f$ = 0.3 mm/rev; (b) No. 3, $V_c$ = 2450 m/min, $f$ = 0.3 mm/rev.

Fig. 10 indicate that for low-speed cutting, tensile strain is generated in a thick surface layer, causing the reduction in hardness. In contrast, when the cutting speed is high, a very thin surface layer is intensively strained by compressive stress, while the bulk is less affected. The high strain with compressive stress improves the surface hardness.

As schematically shown in Fig. 11(a), in low-speed cutting ($V_c$< 800 m/min), the tool-workpiece contact time for a certain area of the workpiece surface is long. Therefore, a large portion of the cutting heat flows into the workpiece, causing thermal expansion of the surface layer. After machining, the expanded surface layer cools down and contracts, leaving a tensile residual stress. In high-speed cutting ($V_c$> 1000 m/min), as shown in Fig. 11(b), the tool-workpiece contact time for a certain surface area is so short that almost no heat is conducted into the workpiece, while a large majority of cutting heat flows into the chip [10]. For this reason, the thermal effect on residual stress formation in the workpiece surface is insignificant, and instead, the mechanical effect dominates the residual stress formation. The rubbing effect of the cutting edge causes tensile deformation in the workpiece surface layer during cutting. After cutting, the tensile deformation is restored by the bulk, causing a highly strained layer with compressive residual stress in the gear surface.

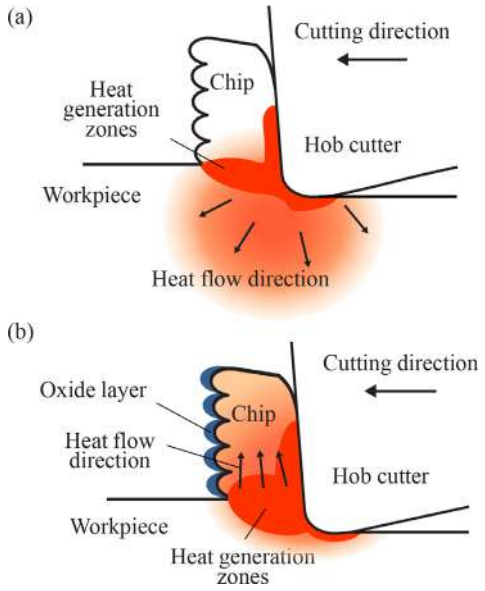


**Fig. 11.** Schematic models for heat flow directions at different cutting speeds: (a) low cutting speed, (b) high cutting speed.

### 3.8. Cutter edge observation

Cutter edge chipping at the early stage of cutting is a major cause of failure in carbide cutters [11]. In this study, the cutter edges of the two hob cutters were observed after hobbing 10 gears. As the wear rate depends on the tooth location of the cutter [12], both the observed teeth were located at the middle parts of the hob cutters. As depicted in Fig. 12, the cutter edges are smooth without big cracks and wear lands. The insignificant tool wear could be attributed to the extremely short contact time between the cutter tip and workpiece at an ultra-high cutting speed, which reduced the thermal damage. Another reason might be that the axial feed used in this study was relatively small, which reduced the cutting force [13]. i.e., the impacting force on the tool tip.

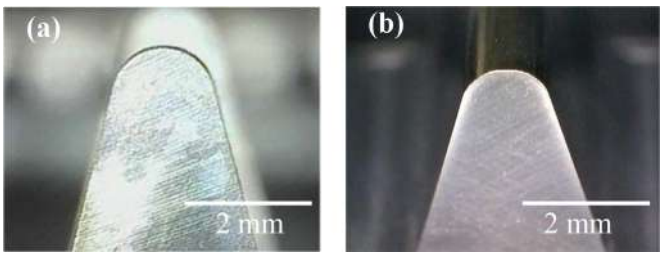


**Fig. 12.** Optical images of tool tips of two hob cutters after hobbing ten gears: (a) 65 mm cutter, (b) 130 mm cutter.

## 4. Conclusions

Gear hobbing experiments were conducted at an ultra-high cutting speed up to ~2450 m/min using a cemented carbide hob cutter, and the machining mechanisms were investigated. It was found that a large majority of cutting heat flew into the cutting chips, causing severe oxidization of the chip surfaces. However, the gear surface was almost unaffected due to insufficient time to conduct heat to the workpiece. Compressive residual stress was generated on the gear surfaces that had improved surface hardness and low surface roughness (~0.1 $\mu$m Ra). The feasibility of improving the productivity and surface integrity of gears by ultra-high-speed hobbing was demonstrated.

## Declaration of Competing Interest

The authors declare that they have no known competing financial interests or personal relationships that could have appeared to influence the work reported in this paper.

## References

[1] Bouzakis KD, Lili E, Michailidis N, Friderikos O (2008) Manufacturing of cylindrical gears by generating cutting processes: a critical synthesis of analysis methods. *CIRP Ann Manuf Technol* 57(2):676–696.
[2] Klocke F, Löpenhaus C, Sari D (2016) Process concepts for gear finish hobbing. *Procedia CIRP* 41:875–880.
[3] Kuljanić E (1985) A method for optimization of hobbing. *CIRP Ann Manuf Technol* 34(1):75–78.
[4] Karpuschewski B, Knoche HJ, Hipke M (2008) Gear finishing by abrasive processes. *CIRP Ann Manuf Technol* 57(2):621–640.
[5] Kizaki T, Katsuma T, Ochi M, Fukui R (2019) Direct observation and analysis of heat generation at the grit-workpiece interaction zone in a continuous generating gear grinding. *CIRP Ann Manuf Technol* 68(1):417–422.
[6] Karpuschewski B, Beutner M, Wengler M, Köchig M (2014) High speed gear hobbing with cemented carbide hobs. *MM Sci J* : 527–532.
[7] Karpuschewski B, Beutner M, Köchig M, Wengler M (2017) Cemented carbide tools in high speed gear hobbing applications. *CIRP Ann Manuf Technol* 66 (1):117–120.
[8] Saria D, Troß N, Löpenhaus C, Bergs T (2019) Development of an application-oriented tool life equation for dry gear finish hobbing. *Wear* 426-427:1563–1572.
[9] Kagawa M, Nishimoto K (1990) A method for evaluating the residual stress from hardness variations - correlation of elastic stress and Vickers microhardness. *J Jpn Soc Precis Eng* 56(9):128–134.
[10] Hirao M, Terashima A, Joo HY, Shirase K, Yasui T (1998) Behavior of cutting heat in high speed cutting. *J Jpn Soc Precis Eng* 64(7):1067–1071.
[11] Bouzakis KD, Antoniadis A (1988) Optimal selection of machining data in gear hobbing regarding the tool mechanical stresses occuring during the cutting process. *CIRP Ann Manuf Technol* 37(1):109–112.
[12] Bouzakis KD, Antoniadis A (1995) Optimizing of Tangential tool shift in gear hobbing. *CIRP Ann Manuf Technol* 44(1):75–78.
[13] Azvar M, Katz A, Van Dorp J, Erkorkmaz K (2021) Chip geometry and cutting force prediction in gear hobbing. *CIRP Ann Manuf Technol* 70(1):95–98.